



OPTIMIZATION OF PROCESS PARAMETERS IN V-GROOVED SOLAR SIMULATOR (COLLECTOR) WITH SEMI-CIRCULAR HEAT PIPE (SCHP)

M. SARAVANAN* and N. KARUNAKARAN

Department of Mechanical Engineering, Annamalai University,
ANNAMALAI NAGAR – 608002 (T.N.) INDIA

ABSTRACT

V-Grooved solar simulator (VGSS) was designed and constructed at Measurements lab of Annamalai University and its thermal performance were analyzed on an indoor test facility. Integrating the V-Grooved absorber plate with flat plate collector can enhance the system performance. VGSS system uses semi-circular heat pipe of length 900 mm and radius of 12 mm. The parameters considered in this analysis are heat input, angle of inclination and flow rate of water in condenser section. The Box-Behnken Design (BBD) Matrix and Response Surface Method (RSM) are applied in designing the experiments to evaluate the thermal resistance and efficiency of the VGSS integrated with semi-circular heat pipe. The experimental results shows that the proposed model will be useful to predict the thermal efficiency of the semi-circular heat pipe within the error of 1%. Therefore the proposed model is useful to predict the thermal efficiency and resistance of semi-circular heat pipe.

Key words: Solar simulator, Heat input, Inclination angle, Flow rate, Thermal resistance, Efficiency, RSM.

INTRODUCTION

Renewable energy has been in the center of attention in recent years due to increasing need of energy. The exhaustion of conventional energy resources and the serious problems caused by environment pollution are the main reasons for using various sustainable green energy resources. In search of renewable and clean energy technology, solar collector has been proved to have promising applications in water heating, refrigeration, water desalination, space heating/cooling, heat pumps, combined energy supply, etc.¹ It is reported that both in developed countries and developing countries solar water heating technology can be one economical choice for its simplicity as a renewable source. Flat plate

* Author for correspondence; E-mail: msapme@gmail.com

collectors have been in service for a long time without any significant changes in their design and operational principles² typically, conventional solar collectors (SC) use water pipes attached to the collecting plate where water circulates either naturally or forcibly and transfers the heat it collects to a storage tank. Some of the shortcomings of this type of solar collector systems include: The additional expense of a pump and the power to operate it; the extra space required for any natural circulation system; the corrosive effect of water; and the limited quantity of heat transferred by the fluid. Heat pipes offer a promising solution to these problems. The heat pipe is a device of very high thermal conductance; that is, it will transport energy without an appreciable drop in temperature³. The heat pipe is suitable for a wide range of applications including solar collector. Thus, solar collectors with heat pipes have a lower thermal mass, resulting in a reduction of start-up time⁴. Thermal diode is important in designing of solar collectors, where heat is transferred only from the evaporator to the condenser, but never in the reverse direction. This feature can cut off the heat loss when the absorber temperature is lower than that of the liquid in the heat exchanger⁴⁻⁷. Several studies on heat pipe solar collectors are reported in the literature. Riffat et al.⁴, studied developing a theoretical model to investigate thermal performance of a thin membrane heat-pipe solar collector. In their work thin membrane heat pipe solar collector was designed and constructed to allow heat from solar radiation to be collected and showed it has high efficiency while keeping the capital cost low. Azad⁸ investigated the heat pipe solar collector theoretically and experimentally, and gave the optimum ratio of heated length-cooled length of the heat pipe. Hull⁹ investigated heat transfer factors and thermal efficiency for heat pipe absorber array connected to a common thermal conductance; that is, it will transport energy without an appreciable manifold and predicted that an array with less than ten heat pipes have significantly less efficiency than conventional flow through collector. Hussein¹⁰ investigated the different design parameters of the natural circulation two phase closed Thermosyphon flat plate solar water heaters using the verified expanded model. Saravanan and Karunakaran¹¹ investigated the V-type absorber plate solar collector with heat pipe shows great potential in terms of higher absorption per unit area as compared to other conventional solar collectors. The solar simulators have been used to investigate the performance of solar collectors in controlled and standard experimental condition. In fact, it provides an effective and repeatable condition to test the performance of the solar thermal collectors. Commercial lamps are applied in solar simulators so as to be capable of providing an environment that is similar to daily changes of radiated sunlight especially in course of illumination and temperature. An environment recreation laboratory can be installed indoor or outdoor. Then, performance and efficiency of the collectors are examined within an artificial environment in the laboratory that is similar to the conditions of natural environment. A solar simulator uses lamp to simulate sunlight. However, lamp cannot create all wavelengths of sunlight¹². For comparative goals, indoor tests are an appropriate and

quick way to achieve results. In 2001; institute for solar energy (ISE) has designed and installed a solar simulation system for indoor solar thermal testing. In fact, outdoor test condition was simulated by indoor test facility to complement the real condition out¹³. The installed solar simulator was enabled to evaluate the performance of solar thermal collectors. Anon and Chaya¹⁴ constructed four single-LED simulators and one multi-color simulator for characterization of solar cells. They obtained high irradiance by employing high pulsing voltages to LEDs. Results from red and blue LED simulators were in good agreement by using correction methods of the IEC891 standard. Bancha et al. used a 1000W halogen lamp as heat source to stimulate solar radiation on Stirling engine. They have measured radiation intensity at various distances to evaluate the performance of solar simulator¹⁵. The real flux distribution has been studied by experimental characterizations of solar simulator. High flux solar simulator was used for controlling conditions and conducting high –temperature and thermo chemical research. The construction of 84 kW solar simulator with an array of 12 xenon –arc lamps and silicone-on-glass Fresnel lenses as the optical concentrator was reported by Wang et al.¹⁶ Manikandan and Sivaraman¹⁷ performed a study on double glazed flat plate solar water heater with different geometries of absorber plates such as Flat, V-groove and Square pulse subjected to uniform mass flow rate. Flat absorber geometry give better results compared to other geometries. This paper analyse the experimental work done and the prediction of empirical relations for heat output, thermal resistance and thermal efficiency of V-Grooved solar simulator/collector using response surface methodology, at real conditions with a system installed at indoor conditions. Response surface methodology is a collection of Mathematical and statistical techniques useful for modeling and analysis of problems in which response of interest is influenced by several variables and the objective is to optimize the response. An experiment is a series of tests, called runs, in which changes are made in input variables in order to identify the reasons for changes in the output responses. Senthil Kumar and Karthikeyan¹⁸ made the analysis of heat pipe operating parameters using copper nano fluid as working fluid based on Box Behnken Design. They analysed various factors such as heat input, angle of inclination, concentration of copper nano fluid and flow rate over the output response of thermal efficiency of heat pipe. The results show that the errors between experimental and predicted values are less than 6%. Manikandan and Senthil Kumar¹⁹ analysed the various parameters that affects the diameter of heat pipe using Central composite design (CCD) and Response surface Methodology. They are applied in designing the experiments to evaluate the interactive effects of the operating variables to evaluate the diameter of heat pipe. The results show that the proposed model will be useful to predict thermal efficiency of heat pipe within the error of 1%. Saravanan and Karunakaran²⁰ analysed the V-Trough solar simulator with heat pipe operating parameters like heat input, angle of inclination and mass flow rate of cooling water by response surface methodology (RSM) on the performance of Copper Deionised water heat pipe with wire mesh screen

wicks. From the mathematical results and RSM optimization it is concluded experimental setup integrated with circular heat pipe gives higher heat input and overall efficiency with lesser thermal resistance. In this research paper, three levels, Box- Behnken Design (BBD) is found to appropriate for designing the experimental conditions. The experiments are designed based on three levels and three factors with 15 runs. Hence, the aim of study is to determine the relationship among the factors Inclination angle ($^{\circ}$), Heat input (Watts) and Flow rate (ml/min) on the thermal efficiency and resistance for VGSS with SCHP and also find the optimal conditions by RSM.

EXPERIMENTAL

Methods

A prototype of V-Grooved solar simulator (VGSS) with Semi-Circular Heat Pipe (SCHP) was designed and tested at indoor facility of Mechanical measurements lab of Annamalai University is shown in Fig. 1. The specifications of heat pipe and solar collector are shown in Table 1. It comprised mainly of copper heat pipe with outside diameter of 24 mm for semi-circular heat pipe with an evaporator length of 630 mm while the wick consisted of two layers of 100-mesh stainless steel screen fitted to the evaporator section. The semi-circular heat pipe was tied on the V-grooved absorber plate and placed in a flat plate solar simulator. Working fluid used in the heat pipe was Deionised water. Heat input is supplied to the evaporator section of semi-circular heat pipe via solar simulator. The solar simulator consists of 6 Halogen lamps of each 300W capacity attached with concave shape reflector of anodised polished aluminum sheet with proper electrical insulation and lighting system is energised with 230V AC supply using variac and measured using a Wattmeter. As by increasing heat flux to the evaporator section of heat pipe, the working fluid DI water in heat pipe gets heated and vaporized and it moves to the condenser section, the outlet jacket with the water, which converts the vapour into the liquid condensate, and it return back to evaporator section due to the capillary action of wicks present in heat pipe. The surface temperature of semi-circular heat pipe, absorber plate and glass plate temperatures was measured using eight K-Type thermocouples once in 20 minutes until the system reaches the steady state condition. Once the steady state condition is attained, the heat input given to the system is stopped and the heat pipe is allowed to cooling down. Then the power is increased to next level and the heat pipe is tested for thermal performance. All the thermocouples were connected to the temperature indicator. The uncertainty in temperature measurement was $\pm 0.1^{\circ}\text{C}$. Glass wool insulation was provided below the absorber plate for reducing the conduction losses, the sides of the absorber plate are covered using thermo cool insulator for minimizing the convective losses. The glass plate is used for reducing the radiation losses by reradiating the heat emitted by the absorber plate in the form infrared rays. Number of glass

plates used was one, if not most of solar radiation will get refracted. Solar power meter was used to measure the solar intensity in W/m^2 . Flow to condenser section was controlled by rotometer and flow rate was maintained at 100, 110 and 120 mL/min. The vacuum pressure in the inner side of the heat pipe is monitored by the vacuum gauge, attached to the condenser end of heat pipe.

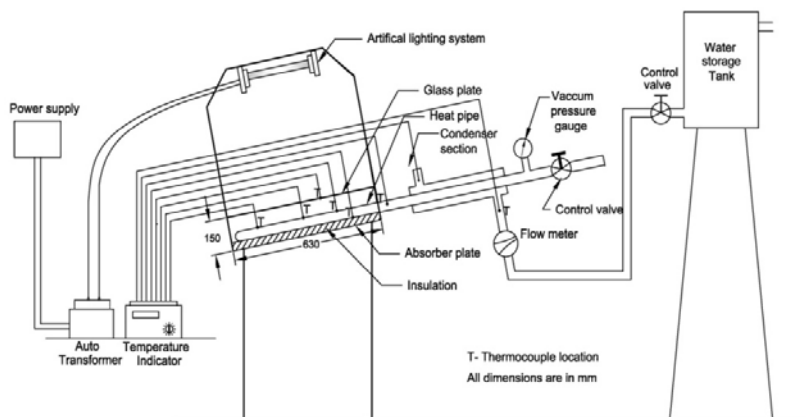


Fig. 1: Schematic diagram of experimental setup

Table 1: Specifications of semi-circular heat pipe and solar collector/Simulator

Heat pipe		Solar collector/Simulator	
Parameters	Specifications	Parameters	Specifications
Length of heat pipe	900 mm	Length of solar collector	630 mm
Evaporator length	630 mm	Breadth of solar collector	400 mm
Adiabatic length	120 mm	Height of solar collector	150 mm
Condenser length	180 mm	Insulation	Mineral wool
Outside diameter of heat pipe	24 mm	Absorber plate material	Copper
Thickness of the heat pipe, t	1.2 mm	Glass plate thickness	3 mm
Mesh number	100	Artificial lighting system	1800W
Wire diameter	0.1 mm	6 Halogen Lamps of 300 W	
No. of layers of wire mesh	2		
Container material	Copper		

Experimental design and data analysis by RSM

Response Surface Methodology (RSM) has several classes of design, with its own properties and characteristics. Box-Behnken Design, Central Composite Design (CCD) and Three Level Factorial Design (TLFD) are the most popular designs applied by the researchers. The Box- Behnken design was used to study the effects of the variables towards their responses and subsequently in the optimization studies. This method is suitable for fitting a quadratic surface and helps to optimize the effective parameters with a minimum number of experiments, as well as to analyse the interaction between the parameters. In order to determine the existence of a relationship between the factors and response variables, the data collected were analysed in a statistical manner using regression. A regression design is normally used in order to model a response as a mathematical function of a few continuous factors. The coded values of the process parameters were determined by the following equation:

$$x_i = \frac{X_i - X_o}{\Delta x_i} \quad \dots(1)$$

where x_i is the coded value of the i^{th} variable, X_i is the encoded value of the i^{th} test variable, X_o is the encoded value of the i^{th} test variable at the center point and Δx_i is the step size. The regression analysis was performed to estimate the response function (Resistance and Efficiency) as a second-order polynomial.

$$Y = \beta_o + \sum_{i=1}^k \beta_i X_i + \sum_{i=1}^k \beta_{ii} X_i^2 + \sum_{i=1}^k \sum_{j=1}^k \beta_{ij} X_i X_j \quad \dots(2)$$

where Y is the predicted response, β_i , β_j and β_{ij} are coefficients estimated from the regression and they represent the linear, quadratic and cross products of x_1 , x_2 and x_3 on response and k is the number of studied factors.

RESULTS AND DISCUSSION

Experiments are conducted by varying the flow rate from 100 to 120 mL/min, Angle of inclination from 30 to 60°, heat input 850 to 1400 W. The surface temperatures are recorded for evaporator and condenser section of heat pipe. The variables flow rate, inclination angle, heat input are chosen as three independent variables in the experiment design. Fifteen trials are conducted to evaluate the effects of these variables on the overall thermal resistance and efficiency which are considered as dependent output variables. Range

and levels of independent process variables for VGSS with SCHP system were given in Table 2.

Table 2: Experimental range and levels of independent process variables for VGSS with SCHP

Parameter	Level		
	-1	0	1
A Heat input, W/m ²	450	900	1350
B Flow rate, mL/min	100	110	120
C Angle of inclination, deg	30	45	60

A statistical program package, "Design Expert 7.15" is used for regression analysis of the data obtained and to estimate the coefficient of the regression equation. The equations are validated by the statistical tests called the ANOVA analysis. The significance of each term in the equation is to estimate the goodness of fit in each case. Response surfaces are drawn to determine the individual and interactive effects of test variables, which are first obtained in coded units and are then converted into the uncoded units.

Fitting models for thermal resistance for VGSS with SCHP

Experiments are performed according to the Box-Behnken experimental design, in order to search for the optimum combination of parameters for obtaining the minimum thermal resistance. The Model F-value of 8.63 implies the model is significant. There is only a 0.48% chance that a "Model F-Value" this large could occur due to noise. The Fisher F test with a probability value as low as 0.0500 demonstrate the significance of the model terms. In this case, A, B, AB, A², B² are the significant model terms. The Goodness of Fit of the model is checked by the Coefficient of Determination (R²). In the present case, R² is calculated as 0.91732. This implies that more than 92 % of the experimental data were compatible with the data predicted by the model and only less than 8% of the total variations are not explained by the model. The R² value always lies between 0 and 1. A statistical model in which the R² value very closer to 1.0 is considered to be an apt model. Here, in this case, the proposed model can be considered as an apt model. The value of Adjusted R² (0.8613) is also high to advocate for the high level of significance of the model. Also, the Predicted R² value (0.7791) is in reasonable agreement with the Adjusted R² (0.8613) value. The value of CV % is also low (3.32), which is an indication of the less amount of deviation between the experimental and predicted values. Adequate Precision is a measure of signal to noise ratio. A ratio greater than 4 is desirable. In this work, the ratio is found to be 10.251

which is a clear indication of the adequacy of the model. The experimental results are analyzed using RSM. The mathematical expression of relationship to the response with variables is

$$\begin{aligned} \text{Thermal resistance} = & +0.12+4.743\text{E-}003 * A+5.971\text{E-}003 * B-1.136\text{E-}003 * \\ & C+3.334\text{E-}003 * A * B-6.868\text{E-}004 * A * C+1.355\text{E-}003 * \\ & B*C -4.128\text{E-}003 * A^2-6.857\text{E-}003* B^2+0.011*C^2 \quad \dots(3) \end{aligned}$$

Where A, B and C are Inclination angle ($^{\circ}$), Heat input (Watts) and Flow rate (mL/min), respectively. The response surfaces and contour plots are generated for different interaction of any two independent variables, while holding the value of the other variable as constant. Such three dimensional surfaces give accurate geometrical representation and provide useful information about the behaviour of the system within the experimental design. The response surface curves for the overall heat transfer coefficient are shown in Figs. 2 to 4.

Table 3: ANOVA for overall thermal resistance

Source	Coefficient factor	F Value	P Value
Model	0.122495	8.632	0.0048
A	0.004743375	10.855	0.0132
B	0.005971	17.201	0.0043
C	-0.001135625	0.622	0.4561
AB	0.003334	2.681	0.1455
AC	-0.00068675	0.114	0.7458
BC	0.001355	0.443	0.5270
A²	-0.004127875	4.327	0.0761
B²	-0.006856625	11.938	0.0106
C²	0.011211625	31.918	0.0008

Standard dev: 4.072E-003; $R^2 = 0.9173$; Adj $R^2 = 0.8111$;
 Predicted $R^2 = 0.7700$; Adequate precision:10.251; C.V.3.32%

Fig. 2 shows the effect of heat input and flow rate on the overall thermal resistance. From the figure, it is observed that an increase in heat input results in a gradual increase of the overall thermal resistance whereas an increase in the flow rate causes a gradual increase

in the overall thermal resistance. Hence, the most influential input parameter among the two is found to be the heat input at evaporator section. Figs. 2 to 4, it is clear that the thermal resistance of heat pipe decreases with increase with the heat input and inclination angle. The thermal resistance valve was minimum at higher heat input and that valve is minimum at 40° to 50° inclination angle. The thermal resistances condense quickly to its minimum valve when the heat load is increased. The lowest overall thermal resistance, within the design profile, is obtained when the heat input and flow rate were maximum.

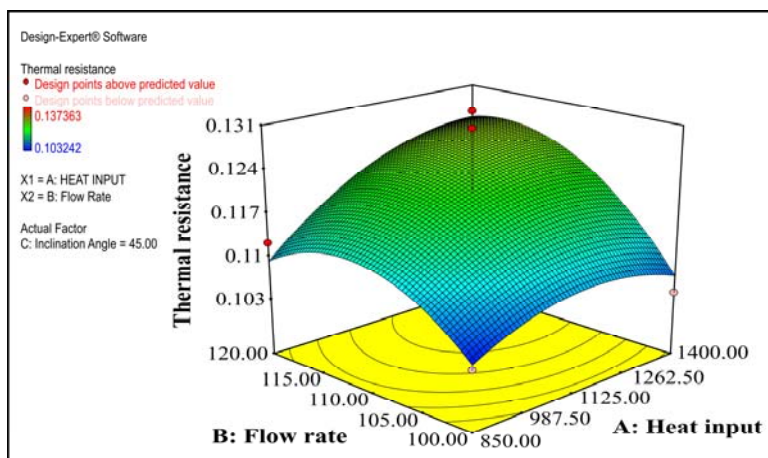


Fig. 2: 3D Plot showing the effect of heat input and flow rate on the overall thermal resistance

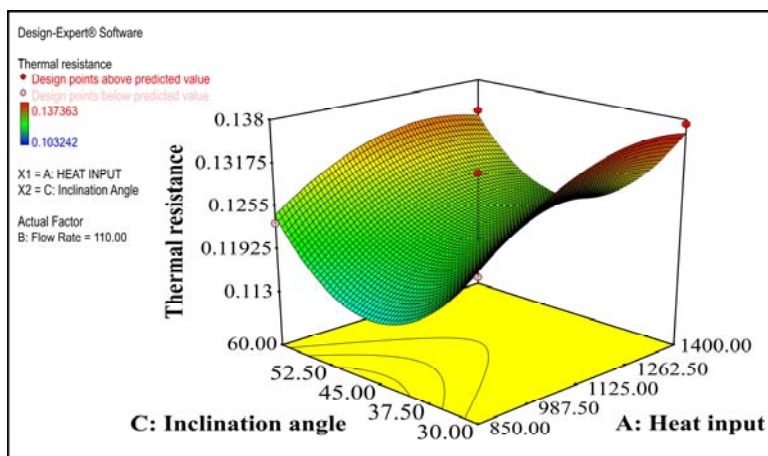


Fig. 3: 3D Plot showing the effect of heat input and flow rate on the overall thermal resistance

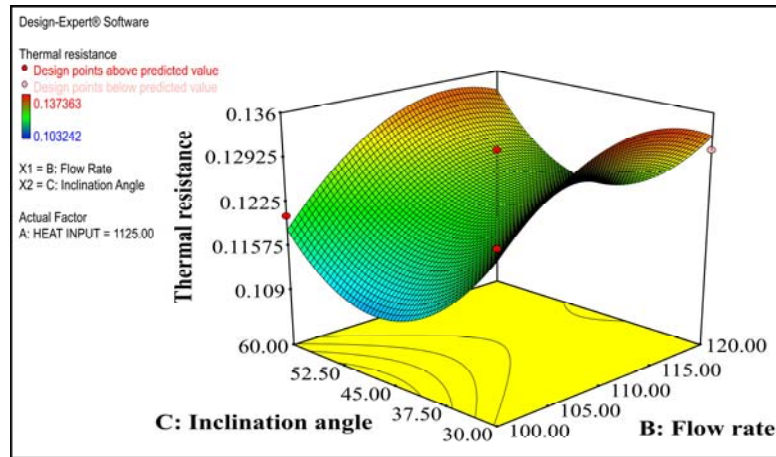


Fig. 4: 3D Plot showing the effect of heat input and flow rate on the overall thermal resistance

Fitting models for thermal efficiency of VGSS with SCHP

Experiments are performed according to the Box-Behnken experimental design as given in Table 2 in order to search for the optimum combination of parameters for maximum efficiency. The Model F-value of 4.34 implies the model is significant. There is only a 3.30% chance that a "Model F-Value" this large could occur due to noise. The Fisher F test with a probability value as low as 0.0500 demonstrate the significance of the model terms. The Goodness of Fit of the model is checked by the Coefficient of Determination (R^2). In the present case, R^2 is calculated as 0.84732. This implies that more than 84% of the experimental data were compatible with the data predicted by the model and only less than 16% of the total variations are not explained by the model. The R^2 value always lies between 0 and 1. A statistical model in which the R^2 value very closer to 1.0 is considered to be an apt model. Here, in this case, the proposed model can be considered as an apt model. The value of Adjusted R^2 (0.7525) is also high to advocate for the high level of significance of the model. Also, the Predicted R^2 value (0.7112) is in reasonable agreement with the Adjusted R^2 (0.7525) value. The value of CV % is also low (6.64), which is an indication of the less amount of deviation between the experimental and predicted values. Adequate Precision is a measure of signal to noise ratio. A ratio greater than 4 is desirable. In this work, the ratio is found to be 7.9521, which is a clear indication of the adequacy of the model. The experimental results are analyzed using RSM. The mathematical expression of relationship to the response with variables is

$$\text{Efficiency} = 26.97 + 3.44 * A - 0.48 * B - 0.47 * C - 1.35 * A * B + 0.29 * A * C$$

$$C+0.60*B*C+1.26*A^2-0.17*B^2-1.54*C^2 \dots(4)$$

Where A, B and C are Inclination angle (°), Heat input (Watts) and Flow rate (ml/min) respectively. The response surfaces and contour plots are generated for different interaction of any two independent variables, while holding the value of the other variable as constant. Such three dimensional surfaces give accurate geometrical representation and provide useful information about the behaviour of the system within the experimental design. The response surface curves for the overall heat transfer coefficient are shown in Figs. 5 to 7.

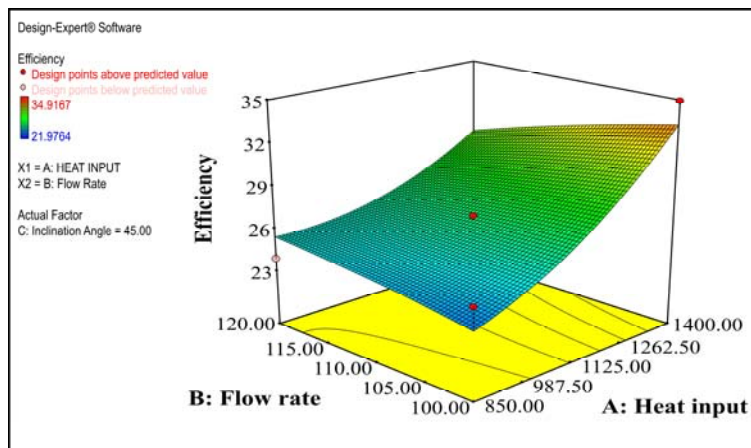


Fig. 5: 3D Plot showing the effect of heat input and flow rate on the overall thermal efficiency

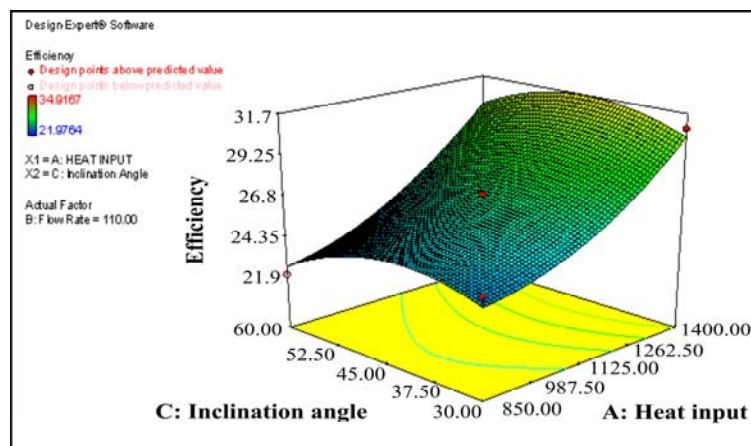


Fig. 6: 3D Plot showing the effect of heat input and inclination angle on the overall thermal efficiency

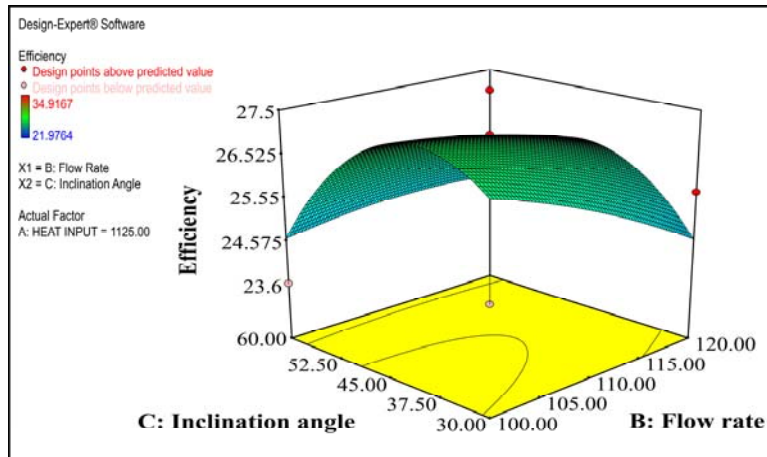


Fig. 7: 3D Plot showing the effect of flow rate and inclination angle on the overall thermal efficiency

Fig. 5 shows the effect of heat input and flow rate on the overall thermal efficiency. From the figure, it is observed that an increase in heat input results in a rapid increase of the overall thermal efficiency whereas an increase in the flow rate causes a gradual increase in the overall thermal efficiency. Hence, the most influential input parameter among the two is found to be the heat input at evaporator section. Figs. 5 to 7, it is clear that the thermal efficiency of heat pipe increases linearly with an increase in heat input at evaporator section. The thermal efficiency of the heat pipe increases with increase in heat flux, due to the fact that the temperature gradient between the evaporator section and condenser sections increase. For higher values of heat input in the evaporator section, the heat generated in the surface is more and the working medium, which is in the form of vapour moves vigorously into the condenser section. The cooling water in the condenser absorbs this excessive heat and as a result, the efficiency of the heat pipe increases.

Table 4: ANOVA for thermal efficiency

Source	Coefficient factor	F Value	P Value
Model	26.9658	4.33869	0.0330
A	3.441363	29.98835	0.0009
B	-0.47734	0.576956	0.4723
C	-0.46805	0.554723	0.4806
AB	-1.3525	2.315987	0.1719

Cont...

AC	0.294075	0.109491	0.7504
BC	0.601175	0.457576	0.5205
A²	1.255075	2.099314	0.1906
B²	-0.17338	0.04006	0.8471
C²	-1.5386	3.154928	0.1190

Standard Dev: 1.78; R² = 0.8473; Adj R² = 0.75251; Predicted R² = 0.7112
Adequate Precision: 7.952; C.V. 6.64%

Confirmation experiments

The Fig. 8 shows the optimization plot generated by the RSM with a desirability of 0.917. It shows that the optimum value of the thermal efficiency is 33.36% and thermal resistance is 0.10743 when the heat input is 1400 W, at 43.68° inclination, and flow rate of water at condenser section is 100.05 mL/min. In order to confirm the optimization results, the experiment is conducted with 1400 W heat input at 45° inclination of the heat pipe with a concentration 100 mL/min. The thermal efficiency of the heat pipe is found as 28.32% and the thermal resistance is 0.129 which is nearer to the optimum value.

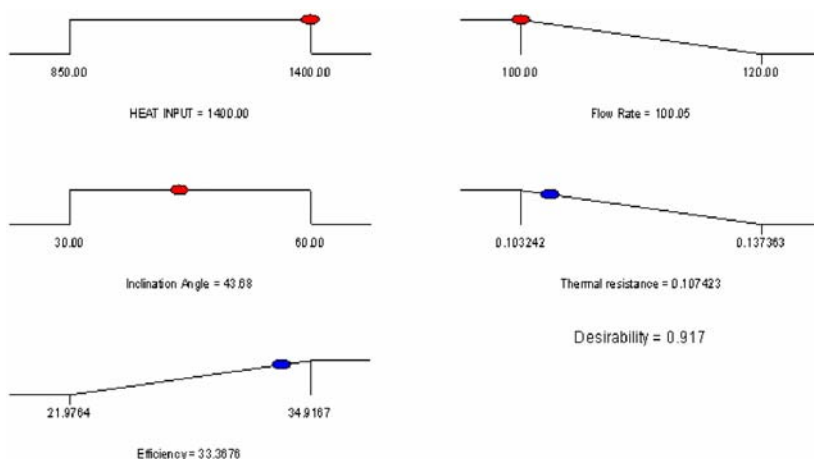


Fig. 8: Optimization plot

CONCLUSION

In this study, RSM is used to determine the optimum operating conditions to get the maximum overall thermal efficiency with minimum thermal resistance in a VGSS with SCHP employing DI water as working fluid in heat pipe. Out of the process variables

considered for evaluation, the heat input, inclination angle and the flow rate are found to be statistically significant. Second order polynomial models were obtained to predict the overall thermal efficiency and resistance. Based on the RSM results, the optimum conditions are found to be: Heat input = 1400 W, Inclination angle = 43.68° and Flow rate = 100.05 mL/min. At these optimum conditions, the maximum efficiency is found to 33.36% and is achieved with a minimum thermal resistance of 0.1074°C/W.

ACKNOWLEDGEMENT

The authors thank the authorities of Annamalai University for providing the necessary facilities in order to accomplish this piece work.

REFERENCES

1. S. A. Kalogirou, Solar Thermal Collectors and Applications Progress, Energy and Combustion Sciences, **30**, 231-295 (2004).
2. S. A. Nada, El-Ghetany, Performance of a Two Phase Closed Thermosyphon Solar Collector with Shell and Tube Heat Exchanger, Appl. Thermal Engg., **24**, 1959-1968 (2004).
3. S. B. Riffat and X. Zhao, A Novel Hybrid Heat Pipe Solar Collector/CHP System, J. Renewable Energy, **29**, 2217-2233 (2004).
4. S. B. Riffat, X. Zhao and P. S. Doherry, Developing of a Theoretical Model to Investigate Thermal Performance of a Thin Membrane Heat Pipe Solar Collector, J. Appl. Thermal Eng., **25**, 899-915 (2005).
5. E. Azad and F. Bahar, An Experimental Study of a Coaxial Heat Pipe Solar Collector, J. Heat Recovery Systems, **6**, 255-258 (1986).
6. J. Facao and A. C. Oliveira, Analysis of a Plate Heat Pipe Solar Collector, Int. Conf. Sustainable Energy Tech. Nottingham, U.K., 28-30 (2004).
7. H. M. S Hussein and H. H. El-Ghetany, Performance of Wickless Heat Pipe Flat Plate Solar Collectors Having Different Pipes Cross Sections Geometries and Filling Ratios, Energy Conversion and Management, **47**, 1539-1549 (2006).
8. E. Azad, Theoretical and Experimental Investigation of Heat Pipe Solar Collector, Experimental Thermal and Fluid Sci., **32**, 1666-1672 (2008).
9. J. R. Hull, Analysis of Heat Transfer Factors for a Heat Pipe Absorber Array Connected to a Common Manifold, J. Solar Energy Engg., **108**, 11-16 (1986).

10. H. M. S. Hussein, Optimization of a Natural Circulation Two Phase Closed Thermosyphon Flat Plate Solar Water Heater, *Energy Conversion and Management*, **44**, 2341-2352 (2003).
11. M. Saravanan and N. Karunakaran, Experimental Analysis of Heat Pipe with V-Trough Solar Collector, *Int. J. Res. Adv. Technol.*, **2**, 19-23 (2014).
12. Lee, Solar Simulator using a Combination of Mercury and Halogen Lamps, US Patent No. 7431466B2 (2008).
13. Z. Christian, Design, Manufacture and Installation of Solar Simulator for Green Laboratory an Pontificia Universidade Catolica De Minas Gerais in Brazil, IN: Solar World Congress (2005).
14. N. Anon and J. Chaya, Determination of Solar Cell Electrical Parameters and Resistances using Collar and White LED-Based Solar Simulators with High Amplitude Pulse Input Voltages, *Renew. Energy*, **54**, 131-137 (2013).
15. M. Qinglong and W. Yuan, Performance of a Twin Power Piston Low Temperature Stirling Engine Powered by a Solar Simulator, *Solar Energy*, **85**, 1758-1767 (2011).
16. W. Wang, L. Aichmayerl, B. Laurmert and T. Fransson, Design and Validation of a Low-cost High-flux Solar Simulator using Frensel Lens Concentrators, *Energy Procedia*, **49**, 2221-2230 (2014).
17. J. Manikandan and B. Sivaraman, Experimental Analysis of Double Glazed Flat Plate Solar Water Heater with Various Absorber Plate Geometries, *Int. Energy J.*, **06**, 151-156 (2016).
18. R. Senthilkumar and M. Karthikeyan, Analysis of Heat Pipe Operating Parameters by Response Surface Methodology using Copper Nanofluid as Working Fluid, *Frontiers in Heat Pipe*, **05**, 1-6 (2014).
19. K. Manikandan and R. Senthil Kumar, Optimization of Heat Pipe Container Diameter using Response Surface Technology, **36**, 113-114 (2015).
20. M. Saravanan and N. Karunakaran, Thermal Characteristics of V-Trough Solar Simulator using Different Profiles of Heat Pipes, *Elixir Mechanical Engg.*, **97**, 41938-41942 (2016).

Revised : 17.10.2016

Accepted : 18.10.2016